Proceedings of IMECE'03
2003 ASME International Mechanical Engineering Congress
Washington, D.C., November 15–21, 2003

IMECE2003-42658

COMPLIANT MECHANICAL AMPLIFIER DESIGN USING MULTIPLE OPTIMALLY PLACED ACTUATORS

Smita Bharti
Graduate Student Research Assistant
Penn State University
Department of Mechanical and Nuclear Engineering
332 Leonhard Building
University Park, PA 16802.

Mary Frecker
Associate Professor
Penn State University
Department of Mechanical and Nuclear Engineering
326 Leonhard Building
University Park, PA 16802.

ABSTRACT

The paper discusses a methodology for designing compliant mechanisms with piezoelectric actuation to obtain maximized deflection and force at output. The focus is on design of compliant mechanisms with multiple optimally placed and sized piezoelectric actuators. Thus the number, length and position of actuators in the body of the compliant mechanism are optimized in addition to maximizing the output deflection and force. Results demonstrate that compliant mechanisms with multiple, optimally placed actuators out-perform those with a single actuator placed at a predetermined location.

INTRODUCTION

Optimal placement of actuators is an important aspect in structural design. By including actuator location as a design parameter during the optimization process along with the objective function and constraints, an optimized structural mechanism with the best active material distribution for a particular output requirement can be obtained.

Research has been carried out to determine optimal actuator placement in areas such as vibration suppression (Fahroo et al., 1997), acoustic control (Padula et al., 1998), thermal deformation control (Kapania et al., 1998), active control systems (Rao, et al., 1991) and truss structures (Chen et al., 1991). Genetic algorithms (Furuya et al., 1996), simulated annealing (Chen et al., 1991), heuristic integer programming (Kapania et al., 1998), and tabu search (Padula et al., 1998) are some commonly used methods for finding optimal actuator locations. In their paper, Aldraihem et al. (2000) address the problem of finding optimal size and location of piezoelectric actuator/sensors on beams. The optimization criterion is based on a beam modal cost and controllability index. Bruant et al. (2001) propose a new approach to find optimal locations of piezoelectric actuators and sensors on actively controlled beam structures. Optimal actuator locations are found by minimizing the mechanical energy integral of the system and optimal sensor locations are found by maximizing the energy of the state output. The approaches mentioned above generally consider optimal actuator placement on structures of predetermined and fixed topology.

Our previous work involved developing optimal topologies of compliant mechanical amplifiers to amplify motion produced from piezoelectric actuators (e.g. Canfield and Frecker, 2000). In our previous work, the design domain consisted of a single actuator placed at a pre-specified location in the topology. The resultant topology guarantees maximized output (either stroke amplification or efficiency) for that particular actuator-amplifier configuration. However, the question remains as to whether higher output deflection could be obtained with a different layout of active and passive material. The current paper discusses a method of carrying out actuator location optimization using the topology optimization methodology. The proposed method optimizes the number of actuators used, their locations and their sizes, while maximizing the output deflection against an external spring. A sample problem has been chosen and is optimized for best active-passive material layout. The resultant optimized topology is compared to the case with a single actuator placed at a pre-specified location in the topology. Results show that using multiple optimally placed actuators gives a considerable improvement in final output.

PROBLEM FORMULATION

In many actuator design problems the structural stiffness which the actuator has to work against is known. In the present formulation this external stiffness is modeled as a linear spring of known stiffness at the output point. The optimization problem is formulated to maximize the deflection of the compliant actuator at output, where the output deflection is equivalent to the Mutual Potential Energy (MPE). MPE is the mutual energy of a structural system under two different states of loading. One of the loads is the input from the actuators and the other is a unit dummy load applied at output in the desired output direction. MPE was chosen as the objective function instead of stroke amplification or geometric advantage (GA) since formulation of GA requires the calculation of input displacement, but in the case of multiple actuators, there are multiple input points. Two materials are available for distribution in the topology, a passive material (e.g., aluminum) and an active (piezoelectric) material. Volume constraints are included on both the passive and active material. The problem formulation is shown in (1),

$$\begin{aligned} \max \quad & MPE = v^T K u \\ \text{s.t.} \quad & A_{active}^T L_{active} \le V_{active} \\ & A_{passive}^T L_{passive} \le V_{passive} \\ & A_{low} \le A \le A_{high} \end{aligned} \tag{1}$$

where u is the nodal displacement vector due to the actuation of the active elements, v is the nodal displacement vector due to a virtual load applied at the output point in the direction of the external spring, K is the global stiffness matrix, A_{active} and $A_{passive}$ are the cross-sectional areas of active (piezoelectric) and passive (Al7075) elements respectively, L_{active} and $L_{passive}$ are the lengths of the active and passive elements respectively, V_{active} and $V_{passive}$ are the upper limits on the volume of active and passive elements respectively, and, A_{low} and A_{high} are the lower and upper limits on design variables, respectively. It should be noted that when including an external spring of specified stiffness at the output point, maximizing the output displacement (MPE) is equivalent to maximizing the output force against the spring.

The design domain is parameterized into a ground structure of truss elements. Truss elements do not support bending and thus are used to model the active elements, since piezoelectric "stack" actuators cannot be allowed to bend due to their possible delamination. For the same reason, pinned joints (2 DOF per node) are used instead of solid, since pinned joints prevent element bending. Topology optimization is accomplished by allowing the cross-sectional areas of each element to vary within pre-specified lower and upper bounds. The elements that reach the lower bound are ignored during the final topology interpretation, since they do not contribute significantly to the results.

Initially the ground structure is composed entirely of active elements. Upon application of the (positive) electric field, each active element expands, i.e. the actuation strain is positive. The resultant strain in each element is the superposition of the positive actuation strain and the positive or negative mechanical strain due to the stiffness of the surrounding elements. The optimization process is based on the concept that those active elements in the ground structure that have negative resultant strain do not contribute to achieving an output deflection in the specified direction, and hence can be replaced by passive truss elements. That is, those elements with negative resultant strain are not effective extension actuators and can be replaced by passive elements. This concept is illustrated in Figure 1. Figure 1 shows a simple topology wherein the desired output deflection in the positive y-direction. Each element in the ground structure is initially set to active. After a number of iterations, elements shown in blue are the active elements which have negative resultant strain. Since the desired output deflection is in the upward direction, a resultant contraction of any of these members will cause the output point to move in the negative y-direction. Thus these elements were replaced by passive elements. The advantage of such a switch is two-fold; the contraction of the elements which adversely affect the output deflection is prevented, and the passive elements provide support to the structure. Following the switch another set of optimization iterations was performed. Thus in the proposed optimization scheme, a two-step optimization is performed where in the first step the ground structure consists of only active elements, and in the second step both active and passive elements are included. That is, the coupled effect of active and passive materials is considered in the second step. From the authors experience, the final resultant output deflection is generally much higher than the output deflection prior to the switch from active to passive. Although this behavior may not be guaranteed for every problem, this switching approach was found to improve the objective function in optimization problems of different design domain sizes. In each case an improvement was observed due to the switch to passive.

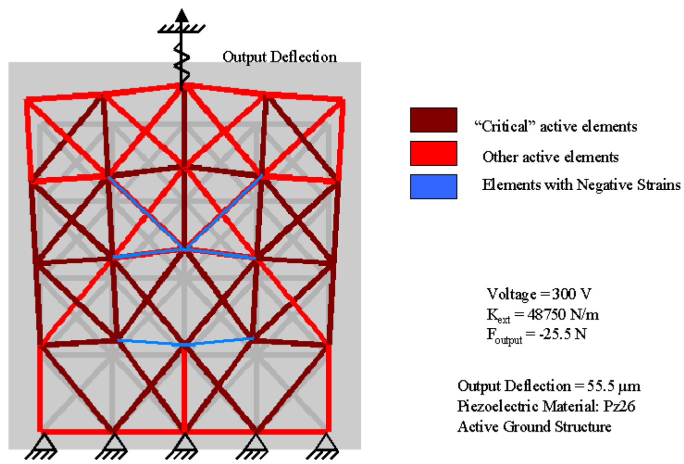

Figure 1. Element with Negative Resultant Strains Replaced by passive Elements.

The topology optimization problem is solved using sequential linear programming (SLP). A linear approximation of the objective and constraint functions is used to approximate the nonlinear objective function, and a small move limit, or step size on the magnitude of changes in the design variables, is used on the update of the design variables so that each iteration results in a small improvement in the objective function.

The solution procedure is shown in Figure 2. The designer supplies the initial size of the design domain, actuator material properties, and passive material properties. The designer also sets parameters for the optimization algorithm such as the lower and upper limits on the design variables, the move limits, and the maximum amount of material or volume the optimizer can use. All elements in the ground structure are initially set to active. The equilibrium equations are solved using standard finite element analysis, and the sensitivities are calculated analytically. The linear sub-problem is solved using the linprog solver in Matlab. The design variables are updated and the process is allowed to iterate a finite number of times (1300 in this case), or until the change in the objective function is very small. Next the resultant element strains are calculated, and the elements that have a resultant strain in a negative direction are switched to passive. Following the switch, the active-passive design is re-optimized for another set of iterations (1300) or until the change in the objective function is very small.

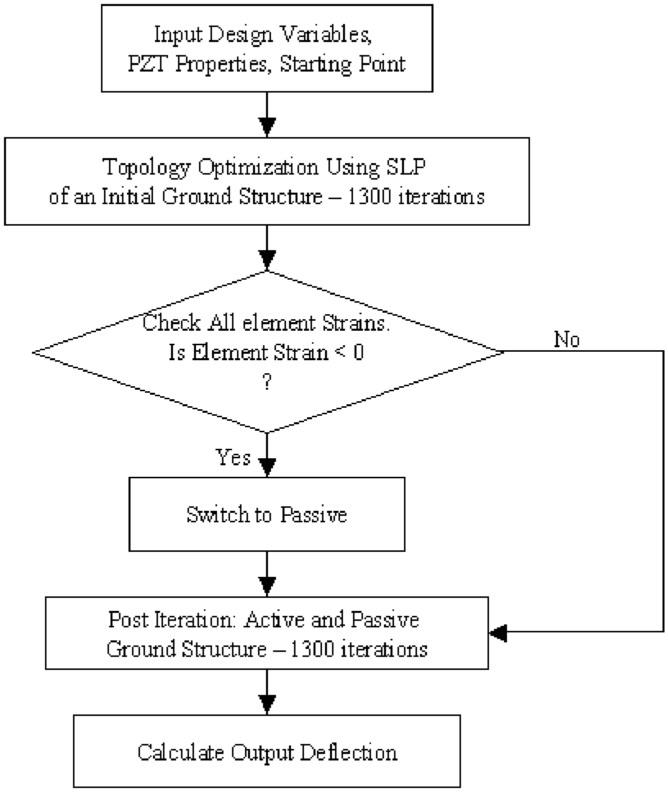

Figure 3. Solution Procedure

EXAMPLE PROBLEM

In order to demonstrate the effectiveness of the method described above, an example problem was solved using this design methodology. In this problem, a 138mm x 28 mm design domain made from an active ground structure of truss elements was optimized. This problem has been taken from our previous work which has been described in detail in Bharti and Frecker (2002) and Brei et al. (2003). A brief review of the problem definition is now given. The problem involved designing a compliant mechanical amplifier for an INertially STAbilized Rifle (INSTAR) with the aim to improve the marksmanship of soldiers under stress during combat by compensating small undesired movements of the barrel. The compliant amplifier was to be used to counter the motion thereby stabilizing the barrel assembly. The design specifications were as follows (see Figure 4). The mechanical amplifier was to reside in a volume of 138mm x 28mm x 35 mm, and was required to provide an output deflection of ±400µm, and an output force of ±19.5 N. In the design procedure used, a spring of stiffness 19.5 N/ 400 µm = 48750 N/m was placed at the output, so that a force of 19.5 N would be obtained automatically when a deflection of 400 µm was achieved. In the earlier design, a single actuator was placed at the center of the design domain and the passive material around it optimized. In the example discussed below, the same design domain is used, but now with multiple optimally placed actuators. A ground structure of 761 elements is used in each case. Al7075 was used as the passive material, and Pz26 from Noliac A/s was used as the active material. The input parameters are given in Table 1 and Table 2.

Table 1. Actuator Properties and Input Parameters

ACTUATOR INPUT PARAMETERS	VALUES
Young's Modulus (E_{pzt})	4.5×10^{10} N/m^2.
Piezoelectric Constant (d_{33})	400×10^{-12} m/V.
Layer Thickness	67 µm
Operating Voltage	300 V
Upper Limit on A_{pzt}	0.0016 m^2.
Lower Limit on A_{pzt}	1×10^{-8} m^2.
Step Size (Maximum allowed change in design variables)	4%
Starting Point of Cross-Sectional Area	0.25×10^{-4} m^2.

Table 2. Other Input Parameters

OTHER INPUT PARAMETERS	VALUES
Total Number of Iterations	2600
Young's Modulus of Passive Material (Al7075)	7.2×10^{10} N/m^2.
External Preload Force	-25.5 N
External Spring Stiffness	48750 N/m

The topology solution for the multiple actuator problem is shown in Table 3. The initial ground structure is shown in light gray in the background, and the topology solutions are shown in their deformed shapes. Active elements that are at or close to the upper limit are shown in dark red. The passive elements are shown in green. Δ_{out} is the actual output deflection while working against the external spring and preload, Force is the corresponding force generated in the external spring, Δ_{free} is the free deflection with no external spring or preload, and $F_{blocked}$ is the blocked force at the output point (i.e., the force generated at zero deflection). In order to determine the equivalent stiffness of the optimized active topology, a unit force is applied at the output in the direction of motion, and the output deflection due to the unit force is determined by carrying out a single optimization iteration with zero voltage. K_{equiv} thus obtained is given by Equation 2.

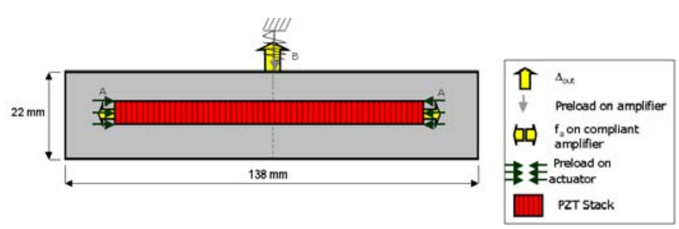

Figure 4. INSTAR Design Problem

$$K_{equiv} = \frac{1}{\Delta_{out}} \qquad (2)$$

Case 1 represents the solution after the first 1300 iterations where all the elements are active, while case 2 shows the final topology once the switch from active to passive has been carried out and the optimization process has been allowed to run for another 1300 iterations. Notice that in the convergence history plot for case 2, a jump in the objective function occurs soon after the switch to passive, demonstrating that the switch to passive does contribute towards obtaining higher output deflection. The final deflections obtained before and after the switch to passive were 1283 μm and 2057 μm respectively.

The output forces obtained before and after switch were 62.54 N and 100.3 N respectively. Free deflection results were obtained by setting the external spring stiffness and the preload force to zero. The resultant free deflection obtained was 1301 μm before the switch and 2102 μm after the switch. Thus the resultant free deflection obtained in multiple actuator optimization was nearly the same as the output deflection obtained with the spring and the preload present, indicating that the solution is very stiff compared to the external spring.

Table 3 also shows the blocked force obtained from constraining the output node from motion. The resultant blocked force obtained before the switch was 6200 N, while the blocked force after the switch was 5921 N, indicating that the topology after switch was more flexible. The equivalent stiffness of the solution was found to be 4,798,465 N/m before and 2,817,060 N/m after the switch. By applying a voltage of –300V on the optimized topology, the output by negative actuation was found to be -2075 μm and –101.2 N (

Table 3, case 3). Volumes of active and passive materials were calculated separately, and a volume constraint of 100% was applied to both active and passive materials.

The same problem was solved for a passive ground structure with a single actuator of pre-specified location. The actuator element was modeled as a single rod element of length 72 mm and cross-sectional area 2×10^{-6} m^2. In this case, the cross-sectional area of the active element is not changed during the optimization. The results are shown in Table 4. The output deflection obtained was 909 μm, which was much lower than the output deflection reported in Table 3 (2100 μm). The output force is 44.3 N. Free deflection and blocked force are 912 μm and 8682 N, respectively. The blocked force is greater than that of the multiple actuator solution, indicating that it is stiffer. This observation is corroborated by the calculation of the equivalent stiffness, which was found to be 9,521,090 N. This was much greater than the equivalent stiffness of the multiple-actuator mechanism (2,817,060 N/m). In this case volume constraint is imposed only on the passive material, since active material is unchanged.

A comparison has also been made for the output work per unit total volume. The results are given in

Table 3 and Table 4. It can be seen that the obtained work per unit volume was about seven times higher in the multiple actuator topology when compared with the single actuator result.

Table 3. Results from Multiple Actuator Optimization

Case	Input Conditions	Optimal Topology	Δ_{out}(μm)	Force (N)	Δ_{free}(μm)	$F_{blocked}$ (N)	K_{equiv} (N/m)	Work/Vol (N/m²)	Convergence History
1	Initial Design Domain: Active V = 300 V 1300 iterations Result before Switch K_{ext} = 48750 N/m $F_{preload}$ = -25.5 N Deformation Magnification = 5 Volume=2.5 m³	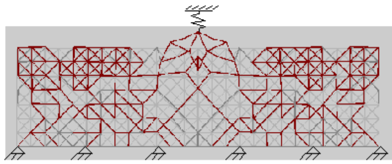	1283	62.54	1301	6200	4798465	0.032	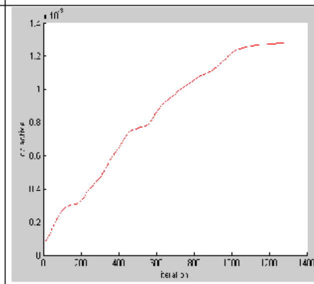
2	Initial Design Domain: Active V = 300 V 2600 iterations Switch to Passive (after 1300 iterations) K_{ext} = 48750 N/m $F_{preload}$ = -25.5 N Deformation Magnification = 5 Volume=2.2 m³	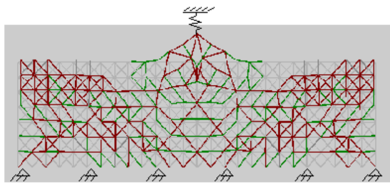 Active Elements Passive Elements	2057	100.27	2102	5921	2817060	0.094	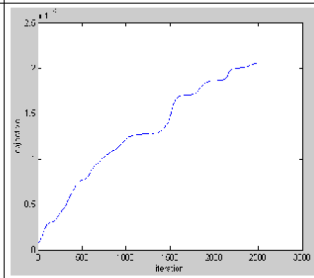
3	Initial Design Domain: Active V = -300 V K_{ext} = 48750 N/m $F_{preload}$ = -25.5 N Deformation Magnification: 2 Volume=2.2 m³	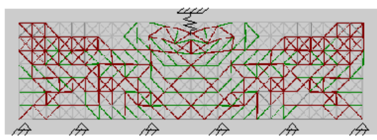 Active Elements Passive Elements	-2075	-101.16	-2102	-5897	2817060	0.095	

Table 4. Results from Single-Actuator Optimization

Case	Input Conditions	Optimal Topology	Δ_{out}(μm)	Force (N)	Δ_{free}(μm)	$F_{blocked}$ (N)	K_{equiv} (N/m)	Work/Vol (N/m²)	Convergence History
1	Initial Design Domain – Passive V = 300 V 1000 iterations K_{ext} = 48750 N/m $F_{preload}$ = -25.5 N Deformation Magnification: 5 Volume=2.8 m³	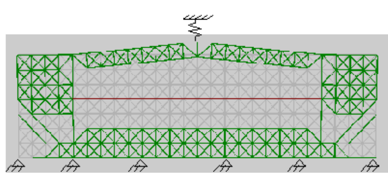 Active Elements Passive Elements	904.6	44.1	912	8682	9521090	0.014	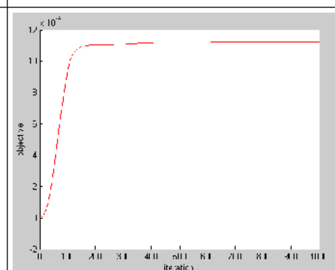
2	Initial Design Domain – Passive V = -300 V K_{ext} = 48750 N/m $F_{preload}$ = -25.5 N Deformation Magnification: 5 Volume=2.8 m³	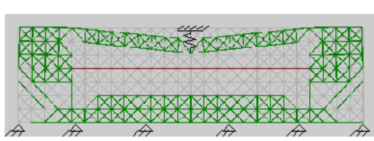 Active Elements Passive Elements	-910	-44.4	-911.9	8680	9521090	0.014	

Table 5: Work Per Unit Volume Comparison

Case	Optimal Topology	Number of active elements	Number of passive elements	Volume Constraint on Active (%)	Volume Constraint on Passive (%)	Switch Criteria (% Strain)	Output Deflection (micron)	Output Force (N)	Work/Volume (N/m^2)
1	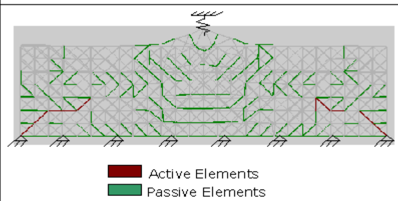	603	159	50	100	0.1	1525	74.34	0.27
2	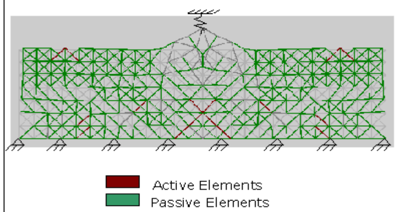	246	516	85	100	1	1865.6	90.95	0.79
3	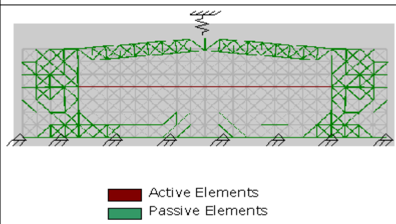	18	744	100	30		919	44.8	0.03
4	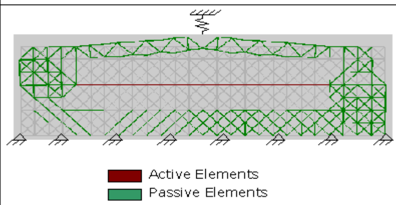	18	744	100	5		871.8	42.5	0.17

Table 5 shows the comparison of work per unit volume of topologies obtained by varying the volume constraints. Case 1 and case 2 are multiple actuator results, while case 3 and case 4 show single actuator results. The multiple actuator solutions out-perform the single actuator solutions, which is not surprising since they contain more active elements. However, it is seen that the multiple actuator solutions still exhibit a higher work per unit volume, though the values obtained are dependent on the volume constraints on active and passive materials as well as the switching criterion as a percentage of strain.

INTERPRETATION

Once the topology solution is obtained it must be interpreted and converted to a solid model of a more practical design. Although the theoretical performance of the topology solution with multiple actuators is quite good, it may be difficult to build if interpreted literally. In an effort to help simplify the solution, several observations can be made about the multiple actuator solution. The first is that there are a large number of active elements, which makes the design very complex. To reduce the number of active elements, several approaches may be taken. One approach is to examine the relative importance of all the active elements, and switch to passive those active elements that are not very close to the upper limit. This approach is illustrated in Figure 4. The elements in blue and the other shades of red are active elements which have areas somewhere between the lower and the upper area limit. These elements could possibly be changed to passive without affecting the output deflection to a great extent. Another way of reducing the number of active elements is to use a lower volume constraint on the active material, or a higher volume constraint on the passive material.

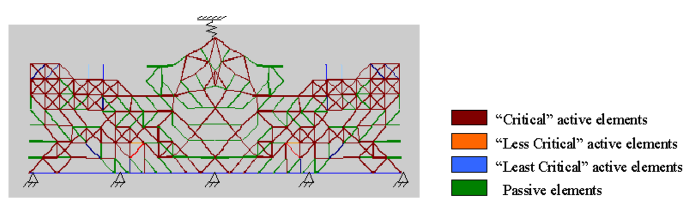

Figure 5. Topology Optimization with all elements shown in different shades according to their relative importance in providing a maximized output deflection.

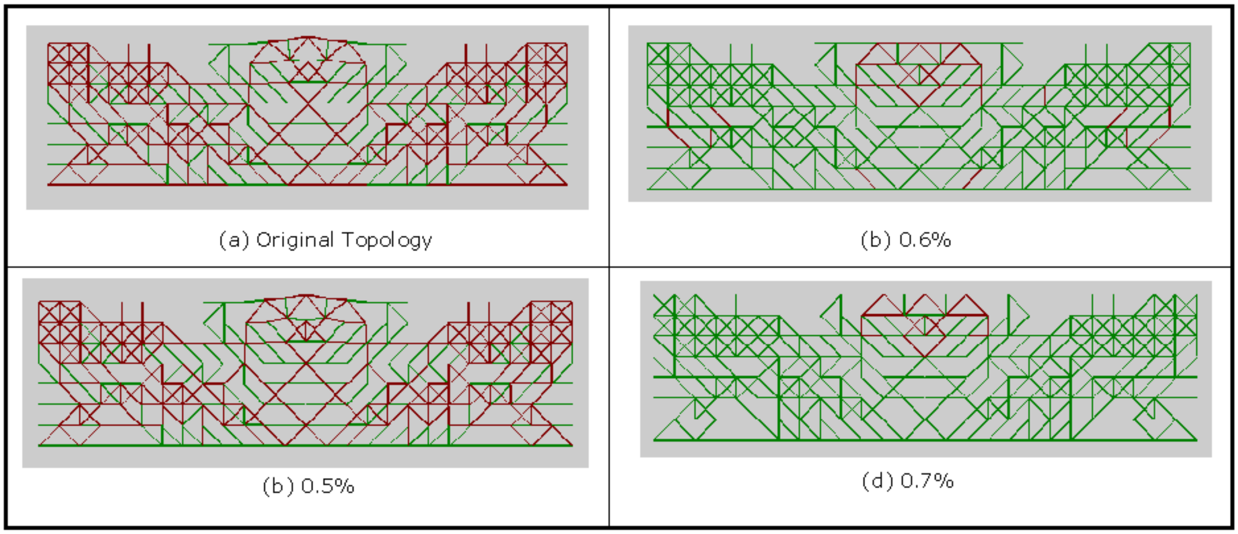

Figure 6. Active Elements below a Threshold Strain Set to Passive

Yet another approach to reduce the number of active elements is to set all elements below threshold strain to passive. Figure 5 shows the results obtained by setting active elements below different threshold strains to passive. Cases b, c and d show topologies obtained by setting elements below 0.5%, 0.6% and 0.7% of the maximum resultant strain to passive. By using different threshold strain values, conclusion about the active elements most important to the topology could be drawn. These are the central elements which remain active in the topology in case 4, when the threshold constraint allows most materials to switch to passive.

Further observations about the multiple actuator solution may help with interpretation. In Figure 6 we see that a group of active elements is concentrated near the upper corners. These sections can possibly be interpreted as one long horizontal actuator on each side near the corners. We also observe a group of active elements near the output point which contribute significantly to the upward output deflection. Thus, a set of vertical actuators could be placed near the output point to imitate the diamond shaped active material layout at the center. Passive material is observed to be concentrated mostly at the center of the design domain.

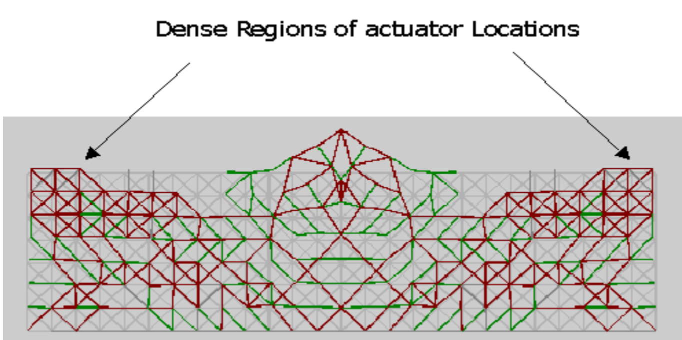

Figure 7. Active Material Concentration

Figure 7 shows a possible interpretation of the topology using a small number of actuators contained in a passive compliant mechanism coupling structure. Using this type of simplified design, it would be relatively easy to do detailed modeling and prototype fabrication. These tasks are beyond the scope of the current paper and will be the focus of future work.

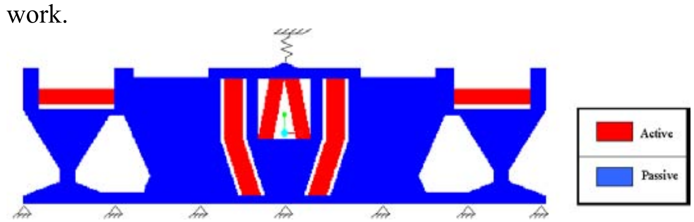

Figure 8. Possible Interpretation

CONCLUSIONS

The approach for designing compliant mechanisms with multiple, optimally placed actuators was shown to be successful in generating topology solutions with good deflection and force performance. The strategy for switching from active to passive based on the resultant element strains resulted in a higher output deflection and force, making it an attractive alternative to using a single actuator in applications where high forces and deflections are required. The final topology obtained, however, is much more complex and difficult to interpret when compared to the single-actuator topology solution. Several strategies for reducing the complexity are suggested. Future work will be focused on interpreting the topology into a solid model and performing detailed finite element analysis.

REFERENCES

Aldraihem, O. J., T. Singh, et al., 2000. Optimal size and location of piezoelectric actuator/sensors: practical considerations. *Journal of Guidance, Control, and Dynamics*, v 23, n 3, May, 2000, pp. 509-515.

Bharti, S., and M. Frecker., 2002. Topology Optimization and Detailed Finite Element Modeling of Piezoelectric Actuators: Effect of External Loads and Detail Geometry on Actuator Output. *SPIE 9th International Symposium on Smart Structures and Materials,* San Diego, California, March, 2002. pp. 124-135.

Brei, D., Vendlinski, J., Frecker, M., and S. Bharti. 2003. Actuation Development and Evaluation for INSTAR – Inertially Stabilized Rifle. *SPIE 10th International Symposium on Smart Structures and Materials*, San Diego, California, March, 2003.

Bruant, I., G. Coffignal, et al., 2001. A methodology for determination of piezoelectric actuator and sensor location on beam structures. *Journal of Sound and Vibration*, v 243, n 5, Jun 21, 2001, pp. 861-882.

Canfield, S. and M. Frecker, 2000. Topology Optimization of Compliant Mechanical Amplifiers for Piezoelectric Actuators. *Structural and Multidisciplinary Optimization,* v 20, n 3, 2000, pp. 269-279.

Chen, Gun-Shing, Robin J. Bruno, Moktar Salama, 1991. Optimal Placement of Active/Passive Members in Truss Structures Using Simulated Annealing. *AIAA Journal*, v 29, n 8, Aug, 1991, pp. 1327-1334.

Ejima, S., Nishiwaki, S., Sekiguchi, M., and N. Kikuchi, 2000. Optimal Structural Design of Compliant Mechanisms Considering a Quantitative Displacement Constraint. *JSME International Journal, Series A*, v 43, n 2, Apr, 2000, pp. 130-137.

Frecker, M., and S. Canfield, 2000. Optimal Design and Experimental Validation of Compliant Mechanical Amplifiers for Piezoceramic Stack Actuators. *Journal of Intelligent Material Systems and Structures*, v 11, n 5, May, 2000, pp. 360-369.

Furuya, H. and R. T. Haftka, 1996. Combining Genetic and Deterministic Algorithms for Locating Actuators on Space Structures. *Journal of Spacecraft and Rockets*, v 33, n 3, May-Jun, 1996, pp. 422-427.

Haftka, R. and Gurdal, Z., 1992. *Elements of Structural Optimization*, 3rd Revised and Expanded Edition, Kluwer Academic Publishers, Boston, MA, 1992.

Kapania, R. K., P. Mohan, et al, 1998. Control of Thermal Deformations of Spherical Mirror Segment. *Journal of Spacecraft and Rockets* 35(2), pp. 156-162.

Lee, T. and I. Chopra, 2001. Design of a Bidirectional Piezoelectric Actuator for Blade Trailing-Edge Flap. *Proceedings of SPIE - The International Society for Optical Engineering*, v 4327, 2001, pp. 36-45.

Nishiwaki, S., Frecker, M., Min, S., and Kikuchi, N., 1998. Topology Optimization of Compliant Mechanisms Using the Homogenization Method. *International Journal for Numerical Methods in Engineering*, v 42, n 3, Jun 15, 1998, pp. 535-559.

Padula, S. L., D. L. Palumbo, et al., 1998. Optimal sensor/actuator locations for active structural acoustic control. *Collection of Technical Papers - AIAA/ASME/ASCE/AHS/ASC Structures, Structural Dynamics & Materials Conference*, v 2, AIAA-98-1865, 1998, pp. 1424-1434.

Prechtl, E., and Hall, S., 1999. Design of a High Efficiency, Large Stroke, Electromechanical Actuator. *Smart Materials and Structures*, v 8, n 1, Feb, 1999, pp. 13-30.

Rao, S. S. and T.-S. Pan, 1991. Optimal Placement of Actuators in Actively Controlled Structures Using Genetic Algorithms. *AIAA Journal*, v 29, n 6, Jun, 1991, pp. 942-943.

Sheng, L. and R. K. Kapania, 2000. Genetic Algorithms for the optimization of piezoelectric actuator locations. *Collection of Technical Papers - AIAA/ASME/ASCE/AHS/ASC Structures, Structural Dynamics and Materials Conference*, v 1, n II, 2000, pp. 1366-1376.

Yousefi-Koma, A. and G. Vukovich, 1996. Shape and Location Optimization of Piezoelectric Actuators in Active Control Systems. *American Society of Mechanical Engineers, Aerospace Division (Publication) AD*, v 52, *Proceedings of the ASME Aerospace Division*, 1996, pp. 559-566.

Fahroo, Fariba and Wang Yun, 1997. Optimal location of piezoceramic actuators for vibration suppression of a flexible structure. *Proceedings of the IEEE Conference on Decision and Control*, v2, 1997, pp. 1966-1971.

